

Experimental verification of the optimal fingerprint method for detecting climate change

Jinbo Hu,^{1,*} Hong Yuan,^{2,*} Letian Chen,^{2,3} Nan Zhao,^{1,†} and C.P. Sun^{2,‡}

¹Beijing Computational Science Research Center, Beijing 100193, People's Republic of China

²Graduate School of CAEP, Beijing 100193, People's Republic of China

³Department of Mathematics and Centre of Complexity Science,
Imperial College London, London SW7 2BZ, United Kingdom

The optimal fingerprint method serves as a potent approach for detecting and attributing climate change. However, its experimental validation encounters challenges due to the intricate nature of climate systems. Here, we experimentally examine the optimal fingerprint method simulated by a precisely controlled magnetic resonance system of spins. The spin dynamic under an applied deterministic driving field and a noise field is utilized to emulate the complex climate system with external forcing and internal variability. Our experimental results affirm the theoretical prediction regarding the existence of an optimal detection direction which maximizes the signal-to-noise ratio, thereby validating the optimal fingerprint method. This work offers direct empirical verification of the optimal fingerprint method, crucial for comprehending climate change and its societal impacts.

Introduction. - The Earth's climate is indispensable for human survival, drawing significant attention to research on climate issues due to its direct impact on both present living conditions and future development. Understanding climate change is vital for creating effective policies and strategies to cope with its effects. However, studying climate change comes with its own set of challenges.

The climate system's complexity, characterized by an array of interacting components, complicates straightforward mathematical representation. For instance, the chaotic nature of temperature evolution, influenced by numerous factors with complex mechanisms, challenges direct modelling. Nevertheless, the scientific community has made substantial progress in this arena[1]. Researchers have devoted considerable effort towards the development of sophisticated climate models, including general circulation models (GCMs)[2–5] and stochastic climate models (SCMs)[6–8]. These models help us understand how the climate responds to both natural events and human activities. However, given that climatology is an observational science, these models are not feasible to experimental verification but instead are validated against observed data only. This raises another pressing issue: how to distinguish human-induced climate changes from natural variability[9].

For this purpose, Hasselmann introduced the optimal fingerprinting method, mathematically represented by the product of the expected signal pattern and the inverse of the climate variability covariance matrix[9–11]. Geometrically, the fingerprint represents a direction minimizing the influence of high-noise components, facilitating the detection of anthropogenic climate signals. Beyond detection, this method is also crucial to identifying the attribution to specific causes[12–19]. Based on this method, the scientists conclude that the human activities indeed impact the climate changes with high confidence[20]. This scientific evidence supports and promotes policy decisions aimed at mitigating climate change through measures like reducing greenhouse gas emissions.

Unfortunately, the inherent complexity of climate systems once again poses significant challenges to the experimental validation of the optimal fingerprinting method. For instance, this method relies on certain assumptions such as the linear su-

perposition of external forces and internal variability effects. The intricate nature of the systems undoubtedly renders the experimental verification of these conditions highly difficult. Despite these obstacles, the method's pivotal role in climate prediction and the profound implications of its conclusions underscore the necessity for its experimental validation.

In this study, we propose an experimentally verifiable system for demonstration. In specific, we consider a *spin resonance system* with noise. Atomic spins are subjected in a well-controlled magnetic field (the external force) and a stochastic magnetic field (the noise). With the adiabatic approximation and rotating wave approximation, the noise-driven part and the external-force-driven part of the measured data are separated. From these two parts of the data, we theoretically calculate the corresponding optimal direction, the fingerprint, under the restriction of maximizing the signal-to-noise ratio. The theory is verified through simulations and experiments. The measured optimal direction matches the theoretical prediction, confirming the validity of the optimal fingerprint method, and providing a solid experimental foundation for the further application of the optimal fingerprint method in climate change detection and attribution.

Optimal fingerprint method[9]. - The optimal fingerprint theory assumes that the observed climate data Ψ (an N -dimensional vector) is a linear superposition of the expected signal Ψ_s , namely, the forced deterministic one, and the noise $\delta\Psi$ of the climate system

$$\Psi = \Psi_s + \delta\Psi, \quad (1)$$

In general, Ψ_s can be predicted by a particular model which describes the climate change response to an external force. $\delta\Psi$ may be treated as a multicomponent Gaussian random variable with zero mean value and known covariance matrix \mathbb{C} . Given an arbitrary vector \mathbf{n} (unnecessarily to be normalized, and referred to as the *measurement direction* hereafter), the square of the signal-to-noise ratio (SNR) along the direction of \mathbf{n} is defined as

$$R^2(\mathbf{n}) \equiv \frac{(\Psi_s \cdot \mathbf{n})^2}{\langle (\delta\Psi_s \cdot \mathbf{n})^2 \rangle}. \quad (2)$$

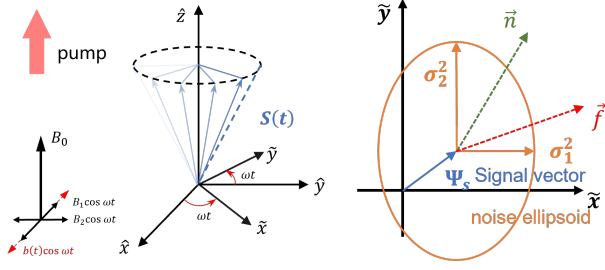


FIG. 1. An illustration of the spin dynamics evolution and the fingerprint method. (a) The evolution of the spin driving by a resonant transverse magnetic field. The spin vector precess (the blue arrows) in the main magnetic field B_0 with frequency $\omega_0 = \gamma B_0$. The spin components can be observed in either the laboratory frame (the $\hat{x} - \hat{y}$ frame) or the rotating frame (the $\tilde{x} - \tilde{y}$ frame). (b) The optimal fingerprint theory in the spin system. The spin signal Ψ is represented by a two-dimensional vector (the blue arrow) in the rotating frame. The orange ellipsoid shows the fluctuation of spin generated by the noise field. Both the signal and noise are projected to the detection direction $\hat{\mathbf{n}}$ to estimate the SNR, which reaches the maximum in the optimal direction $\hat{\mathbf{f}}$.

Let $\hat{\mathbf{n}}_s$ be a unit-length vector denoting the direction of the signal, $\Psi_s = \Psi_s \hat{\mathbf{n}}_s$ with $\Psi_s = |\Psi_s|$ being the magnitude of the signal, the signal Ψ_s can be detected with high level of confidence as long as the SNR along $\hat{\mathbf{n}}_s$ is sufficiently large, i.e., $R^2(\hat{\mathbf{n}}_s) \gg 1$.

However, for a climate system, it is almost impossible to distinguish the expected signal from the natural noise, i.e., the expected signal is undetectable, without using some filtering techniques to eliminate unavailing information. Hasselmann developed the optimal fingerprint method to detect the signal from noise. The optimal fingerprint $\hat{\mathbf{f}}$ is defined as the vector that maximizes the SNR,

$$\hat{\mathbf{f}} = \arg \max_{\hat{\mathbf{n}}} R^2(\hat{\mathbf{n}}), \quad (3)$$

With the covariance matrix \mathbb{C} of the noise vector, the optimal fingerprint $\hat{\mathbf{f}}$ relates to the signal Ψ_s as

$$\hat{\mathbf{f}} = \mathbb{C}^{-1} \Psi_s. \quad (4)$$

Equation (4) shows that the optimal fingerprint $\hat{\mathbf{f}}$ is, in general, unparallelled with the signal Ψ_s . The optimal detection direction is neither along the direction of the maximum of the signal nor the minimum of the noise (see Fig. 1).

Fingerprint in spin system. - We simulate the complex climate system and examine the optimal fingerprint method by a well-controlled magnetic resonance system of spins. The spins now represent the climate system, while the magnetic field represents the external forcing in climate problems. The model used to determine such response is the Bloch equation [21, 22]

$$\frac{d\mathbf{S}}{dt} = -\gamma \mathbf{B} \times \mathbf{S} - \hat{\Gamma} \cdot \mathbf{S}, \quad (5)$$

TABLE I. Comparison between climate system and spin resonance system

	Climate System [9, 10]	Spin Resonance System
dynamics	climate models, <i>e.g., Global Climate Models</i>	Bloch equation
external forcing	human and natural activities, <i>e.g., emissions of greenhouse gases from human activities</i>	magnetic field, <i>e.g., B_x, B_y</i>
signal	climate variables, <i>e.g., global mean surface temperatures</i>	atomic spin
noise	natural internal variability	spin noise induced by the magnetic field noise

where \mathbf{S} is the spin vector, γ is the gyromagnetic ratio, \mathbf{B} is the magnetic field, and $\hat{\Gamma} = \Gamma_2(\hat{x}\hat{x} + \hat{y}\hat{y}) + \Gamma_1\hat{z}\hat{z}$ is the relaxation tensor with Γ_1 and Γ_2 being the longitudinal and transverse relaxation rate respectively [23, 24]. The magnetic field \mathbf{B} consists of a static field $B_z = B_0$ along the \hat{z} direction, which defines the Larmor frequency $\omega_0 = \gamma B_0$ of the spins, and time-dependent fields $B_x(t)$ and $B_y(t)$ along \hat{x} and \hat{y} directions, which drive the precession of the spins. To be specific, we consider the following form of the transverse driving field

$$B_x(t) = [B_1(t) + \delta b(t)] \cos(\omega t), \quad (6)$$

$$B_y(t) = B_2(t) \cos(\omega t). \quad (7)$$

The amplitude of $B_x(t)$ is also modulated by a Gaussian white noise $\delta b(t)$ to simulate the natural noise. The correlation function of $\delta b(t)$ is $\langle \delta b(t) \delta b(t') \rangle = 2D \delta_{\tau_c}(t - t')$, where D characterizes the power spectrum density, and $\delta_{\tau_c}(t - t')$ is a Dirac- δ like function with short correlation time τ_c .

In the weak driving limit, i.e., $B_0 \gg B_1, B_2$ and $\delta \tilde{b}(t)$, the S_z could be treated as a constant, so the observed signal Ψ should be a two-dimensional vector consisting of transverse components of the spin, namely,

$$\Psi \equiv \begin{pmatrix} \tilde{S}_x \\ \tilde{S}_y \end{pmatrix}, \quad (8)$$

where $\tilde{S}_x = \Re\{S_+ e^{-i\omega t}\}$ and $\tilde{S}_y = \Im\{S_+ e^{-i\omega t}\}$ denote the corresponding components in the rotating frame, and $S_+ = S_x + iS_y$ is the spin component in the laboratory frame.

It is worth mentioning that weak driving condition also guarantees the prerequisite of the optimal fingerprint method, namely, the expected signal Ψ_s driven by the external forcing, i.e. $B_1(t)$ and $B_2(t)$, can be separated from the noise signal $\delta\Psi$ driven by $\delta b(t)$. In the resonant case, one obtains the expected signal Ψ_s and the covariance matrix of $\delta\Psi$ as

$$\Psi_s = \frac{\gamma S_z}{2(\Delta^2 + \Gamma_2^2)} \begin{pmatrix} B_1 \Delta - B_2 \Gamma_2 \\ B_1 \Gamma_2 + B_2 \Delta \end{pmatrix}. \quad (9)$$

$$\mathbb{C} = \frac{D \gamma^2 S_z^2}{8 \Gamma_2} \begin{pmatrix} 1 & 0 \\ 0 & 3 \end{pmatrix}. \quad (10)$$

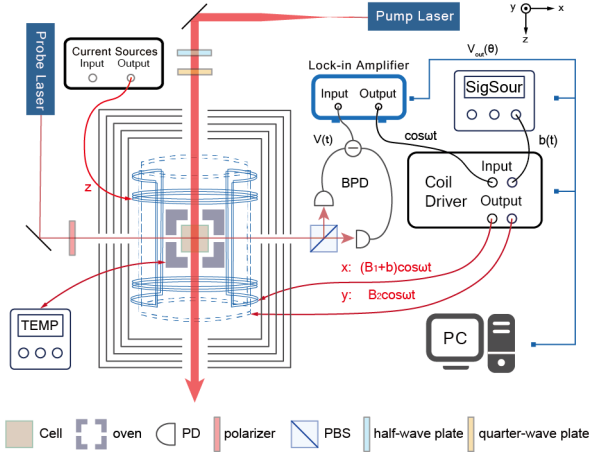


FIG. 2. Schematic illustration of the experiment setup. Atomic spins are polarized and detected by the pump and probe laser beams. The optical signal is converted to an electrical signal by the balanced photodetector (BPD) and analysed and recorded by the data acquisition system consisting of a lock-in amplifier and a computer. The coil driver generates electric current with well controlled amplitude and phase to drive the transverse magnetic field $(B_1\hat{x} + B_2\hat{y}) \cos \omega t$ and the Gaussian noise field $b(t) \cos \omega t$.

According to Eqs. (4) & (10), the optimal detection direction θ_{opt} depends on the driving field amplitudes B_1 and B_2 as

$$\tan \theta_{\text{opt}} = -\frac{B_1}{3B_2}, \quad (11)$$

which indicates the optimal fingerprint detection in the spin system.

The spin magnetic resonance system described by Eqs. (5)-(10) supports a fully controllable physical model to experimentally study the optimal fingerprint method. Various parameters in the spin system, including the relaxation rates Γ_1 and Γ_2 , the noise intensity D , and the driving field amplitudes B_1 and B_2 , are tunable in a wide range to mimic the climate system. Furthermore, the resonance system contains several time scales, including (i) the correlation time τ_c of the noise $\delta b(t)$ is the shortest timescale in the system; (ii) the spin precession period $T_0 = 2\pi/\omega_0$; (iii) the spin relaxation time $T_1 = \Gamma_1^{-1}$ and $T_2 = \Gamma_2^{-1}$ [22–25]; and (iv) the characteristic timescale τ_B of the change of the driving field $B_{1,2}(t)$, which changes vary slowly and is the longest timescale in the system. The hierarchy of different time scales (i.e. $\tau_c \ll T_0 \ll T_{1,2} \ll \tau_B$) mimics the complex dynamic behavior of climate system. Consequently, the spin resonance model is a suitable physical system for verifying fingerprint method.

Experimental verification of fingerprint method. - The experiment setup is illustrated in Fig. (2). A glass cell filled with purified ^{87}Rb atoms and 350 Torr N_2 as buffer gas is placed in an oven, which is heated to 110°C . The atomic density of the Rb vapor at this temperature is $1.2 \times 10^{13} \text{ cm}^{-3}$. The glass vapor cell, the oven and a set of three-axis magnetic field coils are placed in a five-layer magnetic shield to

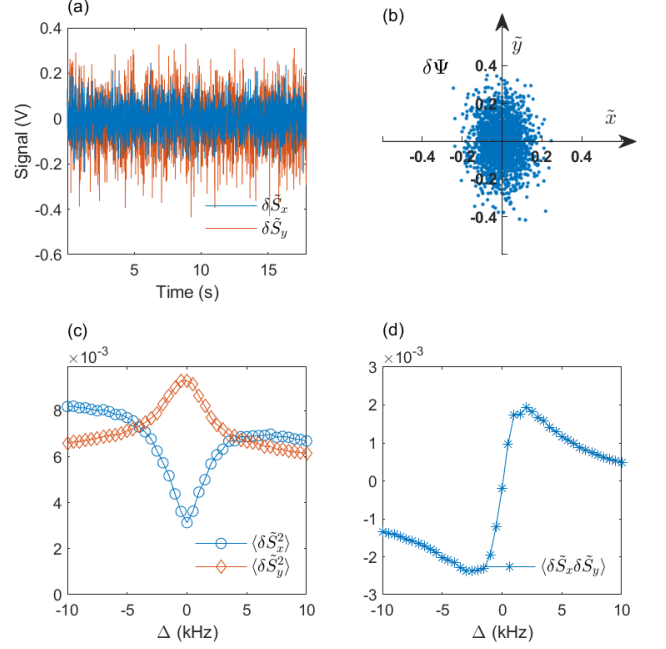


FIG. 3. (a) Measured spin time-domain fluctuation $\delta\tilde{S}_x$ and $\delta\tilde{S}_y$ in the rotating frame. (b) Distribution of the spin fluctuation represented by the vector $\delta\Psi$ in the two-dimensional plain. With the resonance condition ($\Delta = 0$), the distribution is an ellipse with the major axis along \tilde{S}_y direction, and the aspect ratio is 1/3, which agrees with the prediction in Eq. (10). (c) & (d) The variances $\langle \delta\tilde{S}_x^2 \rangle$ and $\langle \delta\tilde{S}_y^2 \rangle$ [the diagonal elements of covariance matrix] and the cross correlation function $\langle \delta\tilde{S}_x \delta\tilde{S}_y \rangle$ [the off-diagonal element of covariance matrix] as functions of the detuning Δ . The detailed calculation can be found in the supplementary.

eliminate the earth magnetic field and the unwanted magnetic noise. The Rb atomic spins are optically pumped by a circular polarized laser beam propagating along the \hat{z} direction in resonance with the D1 line of the Rb transition. The transverse spin component S_x of Rb atoms in lab coordinates is detected by a linearly polarized laser beam along \hat{x} direction via the Faraday rotation effect [25]. A magnetic field $B_0 = 3.5 \mu\text{T}$ is applied along \hat{z} direction, corresponding to the Larmor frequency $\omega_0 = 24.75 \text{ kHz}$ of ^{87}Rb spins. The deterministic amplitudes B_1 and B_2 of the driving field components are generated by the LIA, and the Gaussian noise $\delta b(t)$ is generated by a signal source. These signals are converted to the driving magnetic fields by the coil driver (see Fig. 2).

Experimentally, the signal Ψ is obtained directly by demodulating the voltage $V(t)$ from the balance power detector (i.e. BPD, see Fig. 2) with a reference signal $V_{\text{ref}}(t) = \sqrt{2}e^{-i(\omega t + \theta)}$ via a lock-in amplifier (LIA), where θ is the demodulation phase [26]. Given the phase θ , the demodulation output

$$V_{\text{out}}(\theta) = \Psi \cdot \mathbf{n}(\theta) \quad (12)$$

is equivalent to a projection of the signal vector Ψ along the

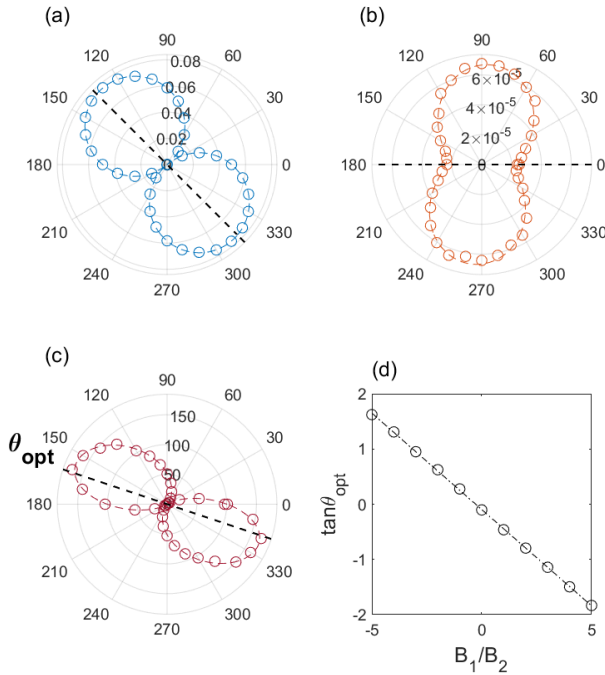


FIG. 4. (a) The spin signal $\langle \Psi_s \cdot \mathbf{n}(\theta) \rangle$ as a function of the detection direction $\mathbf{n}(\theta)$. With amplitude ratio of the driving field set to $B_1/B_2 = 1$, the detection direction which maximized the signal amplitude should be $\theta = 135^\circ$ as shown by the dashed line. (b) The noise amplitude $\langle (\delta \Psi_s \cdot \mathbf{n}(\theta))^2 \rangle$ as a function of the detection direction $\mathbf{n}(\theta)$. The noise amplitude is minimized when the detection is along the \bar{x} axis, the dashed line with $\theta = 0^\circ$. (c) The SNR as a function of the detection direction $\mathbf{n}(\theta)$. The measured data shows the optimal detection direction which maximizes the SNR at $\theta_{\text{opt}} \approx 155^\circ$, which is in good agreement with the theoretical prediction of Eq. (11) as shown by the dashed line. (d) The measured optimal fingerprint (the symbols) as a function of the ratio B_1/B_2 . The dash-dotted line is the theoretical prediction according to Eq. (11)

direction $\mathbf{n}(\theta) = (\cos \theta, \sin \theta)$ in the rotating frame. The fingerprint method is examined by measuring the SNR of the output $V_{\text{out}}(\theta)$ of the spin system as a function of θ . The optimal fingerprint \mathbf{f} in Eq. (4) is indeed the projection direction $\mathbf{n}(\theta)$ which maximizes the SNR.

Figure 3 shows the measured spin signal vector Ψ and its statistical properties under the driving fields $B_x(t)$ and $B_y(t)$ in Eqs. (6) & (7). In the case of resonant driving ($\Delta = 0$), with the demodulation phase $\theta = 0$ or $\theta = \pi/2$, the fluctuation of $\tilde{S}_x(t)$ and $\tilde{S}_y(t)$ induced by the noise field $\delta b(t)$ is obtained, as shown in Fig. 3(a). In the two-dimensional plane spanned by $\tilde{S}_x(t)$ and $\tilde{S}_y(t)$, the distribution of the spin signal vector Ψ forms an ellipsoid with an aspect ratio of $\langle \delta \tilde{S}_y^2 \rangle / \langle \delta \tilde{S}_x^2 \rangle = 3$ [see Fig. 3(b)], which agrees with the theoretical prediction of Eq. (10). The full covariance matrix \mathbb{C} of the spin fluctuation $\delta \Psi$ and its frequency dependence is also measured by varying the driving frequency ω . The variance of $\delta \tilde{S}_y$ ($\delta \tilde{S}_x$) shows a Lorentzian (anti-Lorentzian) lineshape, and the correlation function $\langle \delta \tilde{S}_x \delta \tilde{S}_y \rangle$ is of dispersive profile [Figs. 3(c) & (d)].

Measuring the signal along the \bar{x} or \bar{y} axes is not the optimal choice to extract the signal from the noise. Although the variance of the signal $\langle \tilde{S}_x^2 \rangle$ is small, the signal amplitude along the \bar{x} axis $\langle \tilde{S}_x \rangle$ is also small. By setting the demodulation phase θ , we choose a measurement direction $\mathbf{n}(\theta)$, along which the signal amplitude is a linear combination of $\langle \tilde{S}_x \rangle$ and $\langle \tilde{S}_y \rangle$

$$\langle \Psi_s \cdot \mathbf{n}(\theta) \rangle = \cos \theta \langle \tilde{S}_x \rangle + \sin \theta \langle \tilde{S}_y \rangle, \quad (13)$$

and the variance is

$$\langle (\delta \Psi \cdot \mathbf{n})^2 \rangle = \cos^2 \theta \langle \delta \tilde{S}_x^2 \rangle + \sin^2 \theta \langle \delta \tilde{S}_y^2 \rangle. \quad (14)$$

To find the maximum SNR, we record the signal amplitude and the variance simultaneously while sweeping the measurement direction $\mathbf{n}(\theta)$. As shown in Figs. 4(a) & 4(b), both signal amplitude and variance have their own maximum and minimum values, but they do not coincide in the same direction $\mathbf{n}(\theta)$. According to the fingerprint method, there exists an optimal detection direction $\mathbf{n}(\theta_{\text{opt}})$ which maximizes the SNR. Figure. 4(c) shows the SNR as a function of the detection angle θ , and the optimal detection direction $\mathbf{n}(\theta_{\text{opt}})$ is indicated by the black dashed line.

Figure 4(d) shows the measured the optimal detection direction θ_{opt} as a function of the ratio B_1/B_2 , and the dashed line indicates the theoretical prediction according to Eq.(11). The linear dependence between experiment data and theory agrees well indicating that the fingerprint method in the spin resonance system has been verified.

Conclusion. - In summary, we have experimentally verified the optimal fingerprint method faced on spin system. The spin system is a well-controlled physical model to mimic the complex climate system, and the optimal fingerprint method is examined by measuring the SNR of the output of the spin system as a function of the detection direction. The optimal detection direction θ_{opt} is determined by the driving field amplitudes B_1 and B_2 , and the measured θ_{opt} agrees well with the theoretical prediction. The experimental verification of the optimal fingerprint method in the spin system provides a solid foundation for the application of the optimal fingerprint method in the climate system. Furthermore, the verification makes fingerprint methods becoming a universal and conventional method in solving attribution problems faced on other physical system.

* These authors contributed equally to this work

† nzhao@csrc.ac.cn

‡ suncp@gscaep.ac.cn

- [1] WMO; ICSU; International Study Conference (29 July - 10 August 1974), *The Physical Basis of Climate and Climate Modelling: Report of the International Study Conference in Stockholm, 29 July-10 August 1974*, 16 (World Meteorological Organization, 1975).
- [2] J. Hansen, G. Russell, D. Rind, P. Stone, A. Lacis, S. Lebedeff, R. Ruedy, and L. Travis, *Monthly Weather Review* **111**, 609 (1983).

- [3] S. Weart, *Studies in History and Philosophy of Science Part B: Studies in History and Philosophy of Modern Physics* **41**, 208 (2010).
- [4] S. Manabe and R. T. Wetherald, *Journal of Atmospheric Sciences* **32**, 3 (1975).
- [5] A. Voldoire, E. Sanchez-Gomez, and D. Salas y Méria et al., *Climate Dynamics* **40**, 2091 (2013).
- [6] K. Hasselmann, *Tellus A* **28**, 473 (1976).
- [7] C. Frankignoul and K. Hasselmann, *Tellus* **29**, 289 (1977).
- [8] P. Lemke, *Tellus* **29**, 385 (1977).
- [9] K. Hasselmann, *Journal of Climate* **6**, 1957 (1993).
- [10] K. Hasselmann, Meteorology over the tropical oceans , 251 (1979).
- [11] K. Hasselmann, *Climate Dynamics* **13**, 601 (1997).
- [12] M. R. Allen and S. F. B. Tett, *Climate Dynamics* **15**, 419 (1999).
- [13] A. Ribes, S. Planton, and L. Terray, *Climate Dynamics* **41**, 2817 (2013).
- [14] G. C. Hegerl and G. R. North, *Journal of Climate* **10**, 1125 (1997).
- [15] G. C. Hegerl, H. von Storch, K. Hasselmann, B. D. Santer, U. Cubasch, and P. D. Jones, *Journal of Climate* **9**, 2281 (1996).
- [16] G. C. Hegerl, K. Hasselmann, U. Cubasch, J. F. B. Mitchell, E. Roeckner, R. Voss, and J. Waszkewitz, *Climate Dynamics* **13**, 613 (1997).
- [17] P. A. Stott, M. R. Allen, and G. S. Jones, *Climate Dynamics* **21**, 493 (2003).
- [18] Y. Sun, X. Zhang, F. W. Zwiers, L. Song, H. Wan, T. Hu, H. Yin, and G. Ren, *Nature Climate Change* **4**, 1082 (2014).
- [19] B. D. Santer, C. J. W. Bonfils, Q. Fu, J. C. Fyfe, G. C. Hegerl, C. Mears, J. F. Painter, S. Po-Chedley, F. J. Wentz, M. D. Zelinka, and C.-Z. Zou, *Nature Climate Change* **9**, 180 (2019).
- [20] V. Masson-Delmotte, P. Zhai, S. Pirani, C. Connors, S. Péan, N. Berger, Y. Caud, L. Chen, M. Goldfarb, and P. M. Scheel Monteiro, *Ipcc* (2021).
- [21] F. Bloch, *Phys. Rev.* **70**, 460 (1946).
- [22] W. Happer, *Rev. Mod. Phys.* **44**, 169 (1972).
- [23] S. Appelt, A. B.-A. Baranga, C. J. Erickson, M. V. Romalis, A. R. Young, and W. Happer, *Phys. Rev. A* **58**, 1412 (1998).
- [24] W. Franzen, *Physical Review* **115**, 850 (1959).
- [25] S. J. Seltzer, *Developments in alkali -metal atomic magnetometry*, *Ph.D. thesis*, Princeton University (2008).
- [26] M. L. Meade, *Lock-in amplifiers : principles and applications* (Institution of Electrical Engineers, 1983).